

PAPER • OPEN ACCESS

Tensile properties of 3D printed INCONEL 718 cellular specimens

To cite this article: K Monkova *et al* 2024 *J. Phys.: Conf. Ser.* **2692** 012041

View the [article online](#) for updates and enhancements.

You may also like

- [Mesoscale Electrochemical Performance Simulation of 3D Interpenetrating Lithium-Ion Battery Electrodes](#)
Bradley Trembacki, Eric Duoss, Geoffrey Oxberry et al.
- [Microstructure-sensitive mechanical properties of nanoporous gold: a molecular dynamics study](#)
Jiejie Li, Yuehui Xian, Hongjian Zhou et al.
- [Gyroid structures for 3D-printed heterogeneous radiotherapy phantoms](#)
R Tino, M Leary, A Yeo et al.

PRIME
PACIFIC RIM MEETING
ON ELECTROCHEMICAL
AND SOLID STATE SCIENCE

HONOLULU, HI
Oct 6-11, 2024

Abstract submission deadline:
April 12, 2024

Learn more and submit!

Joint Meeting of
The Electrochemical Society
•
The Electrochemical Society of Japan
•
Korea Electrochemical Society

Tensile properties of 3D printed INCONEL 718 cellular specimens

K Monkova^{1,2,*}, G A Pantazopoulos^{3}, P P Monka^{1,2}, A I Toulfatzis³,
K Lengyelova⁴, S Papadopoulou³**

¹TU Kosice, Faculty of Manufacturing Technologies with a seat in Presov, 080 01 Presov, Slovakia

²TBU in Zlin, Faculty of Technology, 760 01 Zlin, Czech Republic

³ELKEME Hellenic Research Centre for Metals S.A., 320 11 Oinofyta Viotia, Greece

⁴TU Kosice, Faculty of Mechanical Engineering, 042 00 Kosice, Slovakia

*katarina.monkova@tuke.sk; **gpantaz@elkeme.gr

Abstract. The aim of the presented research by the authors was to compare the behaviour of four types of cellular structures under quasi-static tensile stress, while two samples were formed by mono-structures Gyroid 10 % and Diamond 10 %, and the other two types were bi-structures, which were created by combining two single structures (Gyroid 5 % + Gyroid 5 %) and (Gyroid 5 % + Diamond 5 %). The samples were made of Inconel 718 by Direct Metal Laser Sintering technology on an EOS EOSINT M270 machine, and they were heat treated according to AMS 5664 procedure. Tensile tests were performed on an Instron 8802 servo-hydraulic testing machine with a maximum capacity of 250 kN at ambient temperature. The results showed that the maximum load corresponded to the diamond (D) cellular structure (approximately 48 kN), while the minimum load was observed for the gyroid-gyroid (GG) structure (approximately 32 kN).

1. Introduction

Nature has developed architectural porous materials for many situations where density is also low because high stiffness and strength are required. Examples are the beaks and bones of birds, which consist of thin, tough skins attached to a highly porous, cellular core. Architecture the core is complex, with intricately shaped ligaments and density gradients. Although humanity has developed synthetic materials such as metal alloys that are superior to the biological basis materials, cellular architectures developed by humans are much less sophisticated than natural ones. Foams and honeycombs are architectures used almost exclusively today because they can be they are easy to manufacture, although they are far from ideal for many applications. Emergence additive manufacturing technologies enable the production of cellular materials with more complex of architecture and many new architectural materials have been created in the last few years. In parallel, computing power and computational methods have improved sufficiently to allow the design materials and structures with a complex cellular architecture optimized for specific applications. [1-3]

Porous materials have good mechanical properties, thanks to which they are widely used in various sectors and industries. Their high density makes it possible to use them in the aviation industry, where they are most often used in the creation of concrete roads that serve as barriers into which the plane sinks after crossing the braking distance and stops safely. In the case of expensive cars, foams serve as deformation zones, despite their higher price compared to commonly used deformation components.



The low weight allows them to be used not only in the aviation and automotive industries but also in the biomedical and construction industries, where the emphasis is placed on the overall weight reduction of individual parts. For example, covers, spoilers and joints. In the chemical industry, they serve as filters for various liquids, but most often oils and lubricants. [4,5]

Since there are many different types of structures, it is important to know their behaviour and properties under different storage and loading methods. The aim of the presented research by the authors was to compare the behaviour of four types of cellular structures under quasi-static tensile stress to find out which of the investigated structure is the most suitable for tensile-loaded components.

2. Materials and methodology

2.1. Samples description

The virtual models of the samples were prepared in CAD/CAM software PTC Creo 8 with the same criterium of 10 % volume fraction that expresses that only 10 % of the total volume of the sample is filled by material and the next 90 % are air pores. Four types of samples were generated. Two samples Gyroid 10 % and Diamond 10 % types were designed as monostructures and the other two types were bi-structures, which were created by combining two structures (Gyroid 5 % + Gyroid 5 %) and (Gyroid 5 % + Diamond 5 %). Both types of structures belong to the so-called Triply Periodic Minimal Surfaces (TPMS). A minimal surface can be defined as a surface on which, at each point, the two principal curvatures are equal in value but have opposite signs (i.e., there is a mean curvature of zero value at all points). [4] TPMS structures can be mathematically modelled using level-set equations. [6]

The basic cells of the Gyroid and Diamond structures generated for the investigated samples are shown in Fig. 1, while their equations for the geometry description are listed in Table 1.

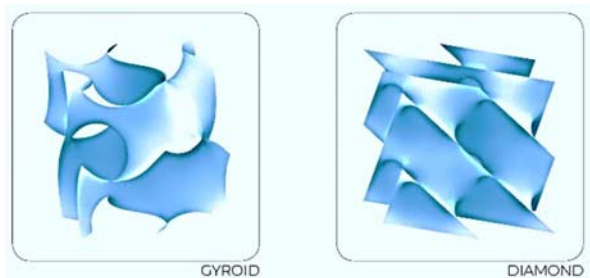




Figure 1. The basic cells of Gyroid and Diamond cellular structures generated for the investigated specimens.

Table 1. Basic equations describing the geometry of single structures (Gyroid and Diamond)

Structure Type	Equation	Cell visualisation
Gyroid	$\sin(x) * \cos(y) + \sin(y) * \cos(z) + \sin(z) * \cos(x) = 0$	
Diamond	$\sin(x) * \sin(y) * \sin(z) + \sin(x) * \cos(y) * \cos(z) + \cos(x) * \sin(y) * \cos(z) + \cos(x) * \cos(y) * \sin(z) = 0$	

One of the advantages of these structures, in addition to their three-periodic geometry, is that they are so-called self-supporting, i.e. they do not need support structures during their production by 3D printing and thus can fill the cavity (core) of a component of any shape without the need to remove the support material, either by dissolving in the case of plastics or blasting in the case of metals. [7-9]

Samples production

The samples were made of Inconel 718 by Direct Metal Laser Sintering technology on an EOS EOSINT M270 machine with a sintered layer thickness of 0.04 mm in one production cycle as a set. All samples were heat treated according to AMS 5664 procedure with inert gas before being removed from the platform. The surface of the samples was finely sandblasted, while the surface roughness showed a Ra value of 12.5 μm . The official name for the material used for additive manufacturing of Inconel 718 is UNS N07718, W.Nr. 2.4668, which is most often known by its tradename Inconel 718. [10,11] This super-alloy belongs to the nickel-based alloys and has special properties which normal materials cannot achieve. These special properties are for example high strength at high and low temperatures (can withstand temperatures up to +700 $^{\circ}\text{C}$), high corrosion resistance at high temperatures, fatigue, creep, etc. [12,13]

A set of the produced samples is presented in Fig. 2.

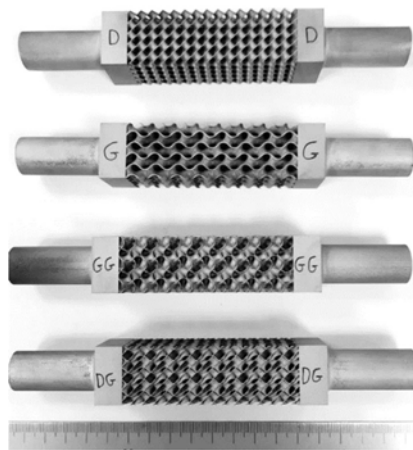


Figure 2. 3D printed INCONEL 718 cellular specimens.

2.2. Samples testing

Tensile tests are essential to ensure operable material of the highest quality that would ensure the functionality, safety and reliability of the designed components. These are important aspects for defining and comparing the properties of materials so that it is possible to prevent unexpected failures and damages closely related to avoid putting non-compliant products into service. These assumptions as well as the right selection of material knowing its properties and behavior in real conditions could keep the end consumer satisfied and dramatically reduce the risk of the components' unexpected failure. [14-16]

Tensile tests within the research were performed on an Instron 8802 servo-hydraulic testing machine with a maximum capacity of 250 kN at ambient temperature using position mode under 1 mm/min cross head speed. The gauge length was setup at 75 mm. The testing set-up for an indicative cellular specimen (Diamond Type) is presented in Fig. 3.

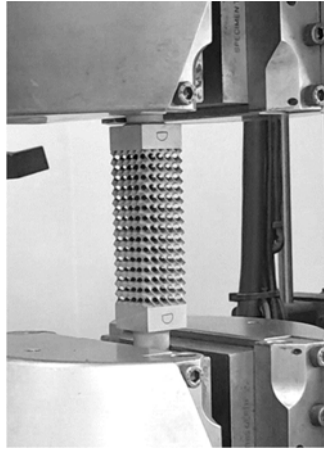


Figure 3. Tensile test set-up for an indicative cellular specimen (Diamond Type).

3. Results and discussion

During the tests, the force load was measured and based on the cross-section area of the samples, the ultimate tensile strength (UTS) R_m was calculated as a ratio

$$R_m \text{ (UTS)} = (\text{Max Load})/(\text{Max Cross Sectional Area}). \quad (1)$$

The tensile test results are presented in Table 2, while force-displacement curves are plotted in Fig. 4.

Table 2. Tensile tests results

No	Sample ID	F_{\max} (N)	R_m (UTS) (MPa)	A (%)
1	Diamond (D)	48460	598	3
2	Gyroid (G)	43874	618	6
3	Gyroid + Gyroid (GG)	31754	418	3
4	Diamond + Gyroid (DG)	39355	458	2

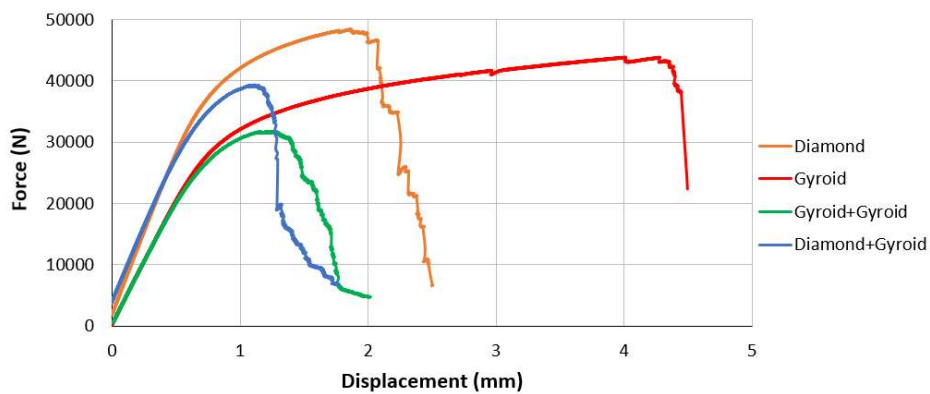


Figure 4. Force-displacement curves obtained after tensile testing.

The maximum load corresponded to the Diamond (D) cellular structure (48 kN approximately) and the minimum load was observed for Gyroid-Gyroid (GG) structure (32 kN approximately).

The order of maximum tensile loads coincides with the results of compression tests of Inconel 718 3D printed cellular materials (peak load values), and it is the following:

$$\text{Diamond (D)} > \text{Gyroid (G)} > \text{Diamond-Gyroid (DG)} > \text{Gyroid-Gyroid (GG)} \quad (2)$$

Several load instabilities (marked as “pop-ins” in Figure 4) indicating locally unstable crack propagation and arrest are demonstrated.

The volume fraction of the samples is controlled by the wall thickness of the structure. Since the bi-structured samples (DG and GG) contain two basic structures with an individual volume fraction $V_f = 5\%$ compared to the mono-structured samples (D and G) where $V_f = 10\%$, the wall thickness of the bi-structured samples is half compared to mono-structured ones. Based on the results presented in Table 1 and equation (2), it can be assumed that the wall thickness plays an important role in the tensile (mechanical) properties of structures.

On the basis of the stress-strain curves, the elastic moduli of the investigated structures were also evaluated. Since all structures had the same volume fraction, it was possible to directly compare other properties such as the modulus of elasticity or ductility. The results showed that the Diamond structure had the best Young's modulus, and the Gyroid structure had the best ductility.

4. Conclusions

There are different types of structures that are stressed in tension. This study is focused on basic research that compares the tensile properties of single and double-arranged cellular porous structures.

Tensile testing was executed at ambient temperature, on four (4) 3D printed INCONEL 718 cellular specimens, manufactured by Direct Laser Metal Sintering (DLMS). The following conclusions can be inferred:

1. The maximum load corresponded to the Diamond (D) cellular structure (48 kN approximately). The order of maximum tensile loads meets the results of compression tests (peak load values),
2. The specimens failed mostly at a plane inclined at around 45° , resulting in a planar/shear fracture surface. The fracture modes highlighted the deformation character of the cellular components showing plasticity behaviour and plateau region of the adjacent walls, predominantly manifested by the Gyroid structure.

Finally, it can be assumed based on the results that the wall thickness plays a very important role in the mechanical properties of the structures and in this case, it is more significant compared to the topology of the sample.

Acknowledgements

The article was prepared thanks to the support of the Ministry of Education of the Slovak Republic through the grants APVV-19-0550, KEGA 005TUKE-4/2021, ERASMUS+ 2021-1-PL01-KA220-HED-000031182 and KEGA 032TUKE-4/2022. The authors also express their gratitude to ELKEME Management team for the continuous encouragement and support.

References

- [1] Gupta, A. et al., Fatigue response of selective laser melted Ti-6Al-4V bracket: an experimental study, *Procedia Structural Integrity* 31 (2021) 15–21.
- [2] Schaedler, T. A., & Carter, W. B. (2016). Architected Cellular Materials. *Annual Review of Materials Research*, 46(1), 187–210. doi:10.1146/annurev-matsci-070115-031624.
- [3] Solberg, K., & Berto, F. (2020). A diagram for capturing and predicting failure locations in notch geometries produced by additive manufacturing. *International Journal of Fatigue*, 134, 105428.
- [4] M. Gavazzoni, M. Pisati, S. Beretta, S. Foletti: Multiaxial static strength of a 3D printed metallic lattice structure exhibiting brittle behavior, *Fatigue Fract Eng Mater Struct.* 2021;44:3499-3516, DOI: 10.1111/ffe.13587.

- [5] Li, W. et al., Effect of high temperature on failure behavior of additively manufactured superalloy under fatigue, *Procedia Structural Integrity* 46 (2023) 119–124.
- [6] Baragetti, S. et al. (2019). Fracture surfaces of Ti-6Al-4V specimens under quasi-static loading in inert and aggressive environments. *Engineering Failure Analysis*, 103, 132–143.
- [7] Bellini, et al.: Manufacturing process effect on the bending characteristics of titanium-lattice/FRP hybrid structures, *Procedia Structural Integrity*, 42, 2022, 196-201, <https://doi.org/10.1016/j.prostr.2022.12.024>.
- [8] Esfarjani, S. M. et al.: Topology optimization of additive-manufactured metamaterial structures: A review focused on multi-material types, *Forces in Mechanics*, 7, 2022, 100100, <https://doi.org/10.1016/j.finmec.2022.100100>.
- [9] Radu, D., Sedmak, A., Sedmak, S., & Li, W. (2020). Engineering critical assessment of steel shell structure elements welded joints under high cycle fatigue. *Engineering Failure Analysis*, 104578. doi:10.1016/j.engfailanal.2020.104578.
- [10] EOS, ‘Material data sheet EOS_NickelAlloy_IN718’, 05-Jan-2023. [Online]. Available: http://ip-saas-eoscms.s3.amazonaws.com/public/4528b4a1bf688496/ff974161c2057e6df56db5b67f0f5595/EOS_NickelAlloy_IN718_en.pdf.
- [11] Daña, M., Zetková, I., Mach J., Mechanical Properties of Inconel Alloy 718 Produced by 3D Printing using DMLS, *Manufacturing Technology*, 18/4, 2018, 10.21062/ujep/137.2018/a/1213-2489/MT/18/4/559
- [12] Kondaa, N., et al., Estimation of high cycle fatigue life of additively manufactured Ti6Al4V using data analytics, *Procedia Structural Integrity* 46 (2023) 87–93.
- [13] M. Gavazzoni, L. Boniotti, S. Foletti: Influence of specimen size on the mechanical properties of microlattices obtained by selective laser melting, *Proc Inst Mech Eng Part C J Mech Eng Sci.* 2019;235(10):1774-1787.
- [14] Nečemer, B. et al.: Fatigue resistance of the auxetic honeycombs, *Procedia Structural Integrity*, 46, 2023, 68-73, <https://doi.org/10.1016/j.prostr.2023.06.012>.
- [15] Dastani, K. et al.: Effect of geometric deviations on the strength of additively manufactured ultralight periodic shell-based lattices, *Engineering Failure Analysis*, 150, 2023, 107328, 10.1016/j.engfailanal.2023.107328.
- [16] Milovanović, N., et al.: (2020). Structural integrity and life assessment of rotating equipment. *Engineering Failure Analysis*, 104561. 10.1016/j.engfailanal.2020.104561